

## *Rhodobacter capsulatus* Genes Involved in Early Steps of the Bacteriochlorophyll Biosynthetic Pathway

ZAMIN YANG<sup>1</sup> AND CARL E. BAUER<sup>1,2\*</sup>

Department of Biology, Programs of Microbiology<sup>1</sup> and Molecular, Cellular and Developmental Biology,<sup>2</sup> Indiana University, Bloomington, Indiana 47405

Received 23 February 1990/Accepted 7 June 1990

Three open reading frames in the *Rhodobacter capsulatus* photosynthesis gene cluster, designated F0, F108, and F1025, were disrupted by site-directed mutagenesis. Mutants bearing insertions in these reading frames were defective in converting protoporphyrin IX to magnesium-protoporphyrin monomethyl ester, protochlorophyllide to chlorophyllide *a*, and magnesium-protoporphyrin monomethyl ester to protochlorophyllide, respectively. These results demonstrate that the genes examined most likely encode enzyme subunits that catalyze steps common to plant and bacterial tetrapyrrole photopigment biosynthetic pathways. The open reading frames were found to be part of a large 11-kilobase operon that encodes numerous genes involved in early steps of the bacteriochlorophyll *a* biosynthetic pathway.

Although the structures of many intermediates in the biosynthetic pathway of chlorophyll *a* and bacteriochlorophyll (BChl) are known (4, 6, 7, 12, 16, 23), many details of photopigment biosynthetic pathways remain obscure. An important approach toward the delineation of these pathways was through the use of mutations that disrupt photopigment biosynthesis at different stages. Early characterization of intermediates in chlorophyll *a* biosynthesis were worked out through the use of mutations in *Chlorella* sp. (11). Similar mutational analysis of the purple bacteria *Rhodobacter sphaeroides* (18) and *Rhodobacter capsulatus* (5, 29, 33) have provided information about intermediates in the BChl *a* biosynthetic pathway. These studies have established that the BChl *a* biosynthetic pathway utilizes intermediates in common with those of the chlorophyll *a* biosynthetic pathway up to chlorophyllide *a* in the following sequence: protoporphyrin IX → magnesium-protoporphyrin → magnesium-protoporphyrin monomethyl ester (MPE) → protochlorophyllide → chlorophyllide *a*. In plant systems, chlorophyllide *a* is phyttylated, resulting in chlorophyll *a*, whereas in the bacterial systems chlorophyllide *a* undergoes additional modifications, ultimately resulting in BChl *a*.

The biochemistry of the enzymatic reactions involved in the photopigment branch of the tetrapyrrole pathway is a particularly limited area of information. Several steps have been shown to exhibit limited *in vitro* activity in plant systems; however, with a few exceptions, there has been little progress in the development of assays for similar reactions that occur in bacterial systems. One of the difficulties appears to lie in the observation that tetrapyrrole intermediates and polypeptides that catalyze these reactions are membrane associated (4, 6, 7, 16, 23, 28), which has hampered the development of techniques for their isolation.

Similarly, there has been little progress in the characterization of genes from plant or bacterial systems that encode enzymes that catalyze (26, 32, 34) or regulate (2) photopigment synthesis. In plant systems, the gene encoding for NADPH-protochlorophyllide oxidoreductase has been cloned and sequenced (26); however, other genes involved in photopigment biosynthesis have not yet been isolated. In

bacterial systems, numerous mutations that disrupt photopigment biosynthesis at different stages have been isolated, mapped, and cloned (5, 19, 29, 33, 36); however, there currently exists sequence information on only two genes that encode for polypeptides involved in later stages Bchl *a* biosynthesis (3, 32, 34). In this study, we utilized site-directed mutational analysis to identify three *R. capsulatus* genes that encode polypeptides involved in early steps of the Bchl *a* biosynthetic pathway. Expression of these genes was shown to be required for the formation of MPE, protochlorophyllide, and chlorophyllide *a* and thus presumably code for enzymes that catalyze early steps in photopigment biosynthesis. The genes identified were also shown to be part of a large 11-kilobase (kb) operon that encodes numerous enzymes in the BChl *a* biosynthetic pathway.

### MATERIALS AND METHODS

**Growth conditions and strain constructions.** Bacterial and phage strains used in this study are listed in Table 1. *Escherichia coli* strains were grown at 37°C in Luria broth (24). *R. capsulatus* strains were routinely grown heterotrophically, photoheterotrophically, or fermentatively in RCV, RCV<sup>+</sup>, PY, PYS, or RCV 2/3 PY medium at 34°C as described previously (5, 31, 34). Mobilization of plasmid derivatives and their selection were performed as described by Young et al. (34) with strains containing the mobilizing plasmid pDPT51 (29). Gene replacement was performed by using gene transfer agent (GTA)-mediated transduction as described by Scolnik and Haselkorn (27) with the GTA-overproducing strain CB1127 (34). Analysis to distinguish between complementation and marker rescue was performed by the sectoring colony technique of Young et al. (34).

**DNA manipulations.** DNA subcloning and transformation into DH5α were performed by using standard procedures (24). For complementation analysis, various plasmids were constructed that contained differing amounts of *Bam*HI fragment D (BamD) DNA upstream from the BamF fragment (Fig. 1, Table 1). Plasmids pCB701 and pUC701 were constructs containing a 3,412-base-pair (bp) region of BamF that included the carboxyl-terminal region of F0 (*bchH*) through the amino-terminal third of the *puhA* gene. These plasmids were constructed by subcloning a 3,412-bp *Bam*HI-

\* Corresponding author.

TABLE 1. Bacterial and phage strains and plasmids

Strain or plasmid	Relevant characteristics	Source or reference
<i>E. coli</i>		
DH5 $\alpha$	F <sup>-</sup> <i>endA1 hsdR17</i> (r <sub>K</sub> <sup>-</sup> m <sub>K</sub> <sup>+</sup> ) <i>supE44 thi-1 recA1 gyrA96 relA1</i> $\phi$ 80 <i>dlacZM15</i>	Hanahan (15)
NM522	<i>supE thi</i> $\Delta$ ( <i>lac-proAB</i> ) $\Delta$ <i>hsd-5</i> (r <sup>-</sup> m <sup>-</sup> )(F <sup>+</sup> <i>proAB lacI</i> <sup>q</sup> $\Delta$ M15)	Gaugh and Murray (9)
Tec5	C600(pDPT51) (mobilizing vector)	Taylor et al. (29)
<i>R. capsulatus</i>		
AJB478	<i>bchB::lacZ</i> <sup>+</sup> 708 <i>crtD233 hsd-1 str-2</i>	Biel and Marrs (5)
AJB480	<i>bchB::lacZ</i> <sup>+</sup> 709 <i>hsd-1 str-2</i>	Biel and Marrs (5)
Bpy4	<i>bchB4 crtF129</i>	Marrs (19)
Brp4	<i>bchE604 crtF129 hsd-1 str-2</i>	Taylor et al. (29)
Brp50	<i>bchH650 crtF129 hsd-1 str-2</i>	Taylor et al. (29)
CB1028	$\Delta$ (F0-F1696)::Km <sup>r</sup>	This study
CB1127	<i>crtG121 rif-10</i> , GTA overproducer	Young et al. (34)
SB1003	<i>rif-10</i>	Yen and Marrs (33)
Y80	<i>bchB80 str-2</i>	Yen and Marrs (33)
ZY4	F1025::Km <sup>r</sup> <i>rif-10</i>	This study
ZY5	F108::Km <sup>r</sup> <i>rif-10</i>	This study
ZY6	F0::Km <sup>r</sup> <i>rif-10</i>	This study
Bacteriophage		
M13mp10		Messing et al. (20)
M13mp11		Messing et al. (20)
M13mp10::F0	<i>Bam</i> HI- <i>Pst</i> I fragment of BamF in mp10	This study
M13mp11::F0	<i>Bam</i> HI- <i>Pst</i> I fragment of BamF in mp11	This study
Plasmids		
pBR322 $\Omega$	$\Omega$ Sp <sup>r</sup> cassette	Prentki and Krisch (22)
pCB701	<i>Bam</i> HI- <i>Xho</i> I fragment from pRPSB104 into <i>Bam</i> HI- <i>Sal</i> I sites of pNM482	This study
pCB701 $\Omega$	$\Omega$ Sp <sup>r</sup> cassette into <i>Bam</i> HI site of pCB701	This study
pCB701D $\Omega$	BamD fragment from pRPSB5 into <i>Bam</i> HI site of pCB701 $\Omega$	This study
pCB701E $\Omega$	<i>Eco</i> RI deletion derivative of pCB701D $\Omega$	This study
pCB701F $\Omega$	<i>Xho</i> I deletion derivative of pCB701D $\Omega$	This study
pCB701D $\Omega$ 0	$\Omega$ interruption of F0 derived from pCB701D $\Omega$	This study
pCB701 $\Delta$ F	F0-F1696 deletion derivative of pCB701F $\Omega$	This study
pNM480	Translational <i>lacZ</i> fusion vector	Minton (21)
pNM482	Translational <i>lacZ</i> fusion vector	Minton (21)
pRPSB104	BamF fragment in pDPT42	Taylor et al. (29)
pRPSB5	BamD fragment in pDPT42	Taylor et al. (29)
PRPSB9	BamI fragment in pDPT42	Taylor et al. (29)
pUC701	pUC9 derivative of pCB701	This study
pUC9	Ap <sup>r</sup> vector	Viera et al. (30)
pUC4-Kixx	Km <sup>r</sup> cassette	Barany (1)
pZY22	F1025::Km <sup>r</sup> derivative of pUC701	This study
pZY32	<i>Sph</i> I deletion derivative of pUC701	This study
pZY33	F108::Km <sup>r</sup> derivative of pZY32	This study
pZY42	F0::Km <sup>r</sup> derivative of pCB701F $\Omega$	This study
pZY62 $\Omega$	F0:: <i>lacZ</i> fusion in pNM480	This study

*Xho*I fragment obtained from pRPSB104 (29) into the *Bam*HI-*Sal*I sites of the polylinkers present in pNM482 (21) and pUC9 (30), respectively. Plasmid pCB701 $\Omega$  contained an additional *Eco*RI restriction fragment termed omega (22) cloned from pBR322 $\Omega$  into the upstream *Eco*RI site of pCB701, located at the vector-insert junction. The omega fragment codes for a spectinomycin resistance (Sp<sup>r</sup>) gene flanked by transcription-translation termination sites and thus serves to protect vector-initiated transcripts from influencing *R. capsulatus* gene expression. Plasmid pCB701D $\Omega$  was a construct that contained the entire 8.0 kb of the BamD fragment obtained from pRPSB5 (29) cloned into the upstream *Bam*HI site of pCB701 $\Omega$ . This latter construction formed a contiguous BamD-BamF region analogous to that in the chromosome. A derivative of pCB701D $\Omega$  termed pCB701D $\Omega$ 0 was constructed in which the upstream omega fragment of pCB701D $\Omega$  was repositioned to the *Bam*HI site at the BamD-BamF junction, thereby disrupting the F0 open

reading frame. Plasmid pCB701F $\Omega$ , which contained 2.5 kb of DNA upstream from the BamD-BamF junction, was constructed by digesting pCB701D $\Omega$  with *Eco*RI and replacing the region that was deleted with the omega *Eco*RI fragment. Plasmid pCB701E $\Omega$  was a construct that contained 4.5 kb of DNA upstream from the BamD-BamF junction. This construct was derived by performing a partial *Eco*RI-*Xho*I digestion of pCB701D $\Omega$  and replacing the region that was deleted with the omega fragment. Additional plasmid constructs are discussed below.

**Site-directed mutagenesis.** Site-directed interposon mutagenesis of F0, F108, and F1025 open reading frames were accomplished by recombining a kanamycin resistance (Km<sup>r</sup>) cassette into the chromosomal copy of each of the respective genes in the wild-type strain *R. capsulatus* SB1003 (33). To reduce the possibility of polarity, we utilized the pUC4-Kixx Km<sup>r</sup> cassette (Pharmacia Fine Chemicals), which contains the Km<sup>r</sup> gene flanked by DNA containing no known tran-

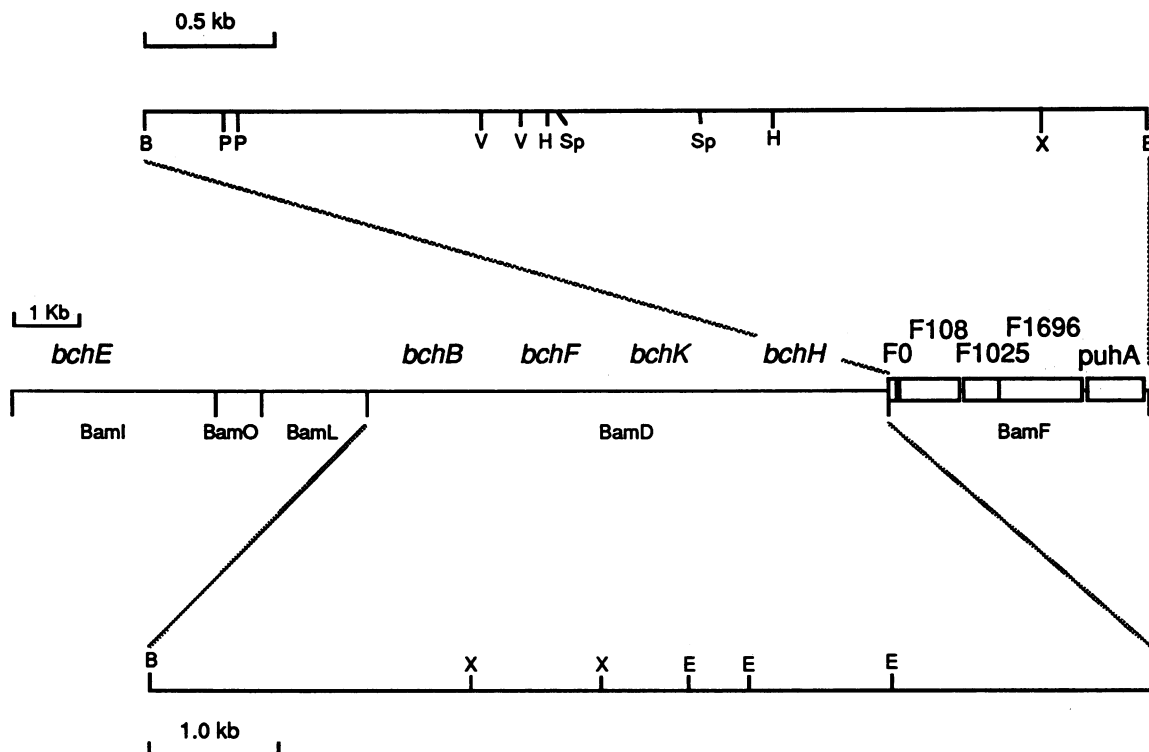


FIG. 1. Restriction and genetic map of the region of the photosynthetic gene cluster analyzed in this study. BamI, BamO, BamL, BamD, and BamF denote differing restriction fragments generated from *Bam*HI restriction digests of the photosynthesis gene cluster (29). The location of the indicated *bch* genes involved in BChl biosynthesis is a compilation of previously published data (5, 29, 35, 36). Restriction sites used in this study are shown in the expanded regions with the following abbreviations for restriction sites: B, *Bam*HI; E, *Eco*RI; H, *Hind*III; P, *Pst*I; Sp, *Sph*I; V, *Eco*RV; X, *Xho*I.

scription termination sites (1). In addition, each of the disruptions discussed below had the  $Km^r$  gene incorporated in the same direction of transcription as the gene with which it was disrupting. Interposon mutagenesis of *F0* was accomplished by inserting the  $Km^r$  cassette from pUC4-Kixx into the unique *Bam*HI site of pCB701F $\Omega$ , creating pZY42. This site is located at the BamD-BamF junction, which disrupts the *F0* open reading frame 25 amino acids from the carboxyl-terminal end. This insertion was subsequently recombined into the chromosome of SB1003 by GTA transduction, creating the strain ZY6.

A 54-bp internal deletion of *F108* was accomplished by using a two-step procedure. The first step involved the removal of a *Pst*I restriction site present in the polycloning site from pUC701. This was accomplished by deleting a 1,821-bp *Sph*I restriction fragment, resulting in the construct pZY32. pZY32 was subsequently digested with *Pst*I, which cuts within *F108* at positions 314 and 368 relative to the start site of BamF, converted to a blunt end with T4 DNA polymerase, and ligated to the *Sma*I-digested  $Km^r$  cassette of pUC4-Kixx, creating pZY33. The  $Km^r$  gene in pZY33 was subsequently recombined into the chromosome of SB1003 by GTA transduction, creating the strain ZY5.

A deletion of *F1025* was accomplished by replacing an internal 156-bp *Eco*RV restriction fragment located within *F1025* (positions 1294 to 1450 relative to the start site of BamF) on the vector pUC701 with the  $Km^r$  *Sma*I cassette of pUC4-Kixx, creating the construct pZY22. This deletion was recombined into SB1003 by GTA transduction, creating the strain ZY4.

A chromosomal deletion extending from the carboxyl-

terminal region of *F0* at the BamD-BamF junction through the amino-terminal portion of *F1696* (position 2424) was constructed by using the plasmid pUC701 $\Delta$ F. This plasmid was constructed by replacing an internal *Bam*HI (position 0)-*Hind*III (position 2424) restriction fragment of pUC701F with the *Sma*I  $\Omega$   $Km^r$  cassette of pHP45 $\Omega$  $Km$ . This was accomplished by filling in the *Bam*HI and *Hind*III overhangs with T4 DNA polymerase before ligation. Upon GTA-mediated transduction of SB1003, the region extending from *F0* through the amino terminus of *F1696* was replaced by the  $Km^r$  gene, creating the strain CB1028.

**DNA sequencing.** DNA sequence analysis of both strands of the *F0-F108* region was performed by first subcloning a 314-bp *Bam*HI-*Pst*I restriction fragment (positions 0 to 314 relative to the *Bam*HI site) from pRPSB104 (29) into similar sites in M13 mp10 and M13 mp11 (20), resulting in the constructs M13 mp10::*F0* and M13 mp11::*F0*. The inserts were completely sequenced by the dideoxynucleotide method (25) with the Sequenase DNA sequencing kit (U.S. Biochemical Corp.). The reactions were resolved by electrophoresis in a 6% polyacrylamide denaturing gel. Analysis of DNA sequence was performed with programs from the sequence analysis package version 6.1 of the University of Wisconsin Genetics Computer Group run on a  $\mu$ Vax computer.

**Northern RNA blots.** Wild-type *R. capsulatus* SB1003 cells were grown under photoheterotrophic conditions in PYS medium (34) to a density of 50 Klett units. The cells were chilled on ice to 4°C and then harvested by centrifugation at 10,000  $\times$  *g* for 15 min at 4°C. The RNA was subsequently isolated in the presence of guanidinium isothiocyanate as

described by Bauer et al. (3). The RNA was separated by electrophoresis in a 1.2% formaldehyde-agarose gel, sheared to smaller fragments by treatment with NaOH, blotted onto a nitrocellulose filter, and hybridized with a  $^{32}\text{P}$ -labeled (multi prime labeling kit; Amersham Corp.) DNA probe as described by Sambrook et al. (24).

**Analyses of tetrapyrroles.** Cells were routinely grown in the dark under low aeration in RCV<sup>+</sup> medium, which is a minimal RCV medium supplemented with 0.6% glucose, 0.5% pyruvate, and 50 mM dimethyl sulfoxide (5). Under low aeration, this medium promotes the production of large amounts of photopigments. Cells were harvested, and pigments were extracted with cold acetone-methanol (7:2) as described previously (5, 8). Spectral and fluorescence scans of tetrapyrroles were performed with a Beckman model DU50 spectrophotometer and a Hitachi F-2000 fluorescence spectrophotometer, respectively (5). Analysis of tetrapyrroles by thin-layer chromatography (TLC) was performed by chromatographing extracted pigments on silica gel G TLC plates (Brinkmann Instruments, Inc.) developed in benzene-ethyl acetate-ethanol (4:1:1) and viewed under long-wavelength UV light as described previously (5).

**Transcriptional analyses.** A translational fusion to *F0* to the *lacZ* structural gene was constructed by cloning the BamD fragment from pRPSB5 (29) into the *Bam*HI site of pNM480 (21), creating the plasmid pZY62. The omega fragment was then inserted at the upstream vector-BamD junction of pZY62, creating pZY62 $\Omega$ . For measuring  $\beta$ -galactosidase activity, the cells were grown in PYS medium either under high-aerobic or photosynthetic conditions, harvested at a cell density of 50 Klett units, disrupted by sonication, and assayed for activity as described previously (3, 34).

## RESULTS

**Open reading frames encoded by the BamF fragment.** A genetic and physical map of the region of the photosynthesis gene cluster analyzed in this study is shown in Fig. 1. In a previous study, Youvan et al. (35) proposed the existence of several open reading frames (ORFs), designated *F108*, *F460*, *F1025*, and *F1696*, encoded by the DNA sequence upstream from the *puhA* gene, which is known to encode the reaction center H polypeptide. They based this proposition on the occurrence of putative ribosome-binding sites located upstream from ORFs. In the current study, we analyzed the DNA sequence of this region with a statistical program for codon utilization (13) by using a codon frequency table generated from *R. capsulatus* genes that are known to be expressed. This program can often identify ORFs that are expressed and can identify DNA sequencing errors due to the inherent bias of codon utilization found in high G+C-rich organisms such as *R. capsulatus*. Analysis of the originally published sequence with this program revealed excellent codon usage for ORFs coding for *puhA*, *F1696*, and *F1025* as well as the possibility of a sequencing error within *F108* (data not shown). The presence of a sequencing error in this region was confirmed by additional sequence analysis (Fig. 2A), which demonstrated that at position 236 the originally reported sequence of GGCAA is actually GGCAA. As a consequence of this correction, the *F108* ORF was shifted in frame with *F460*, forming one large ORF that extended from nucleotide 103 to nucleotide 1019 (Fig. 2B). The existence of this larger ORF was supported by the codon preference plot of the corrected sequence (Fig. 3), which demonstrated excellent codon usage of the corrected *F108* ORF. The

existence of an additional, previously undetected ORF contiguous with the upstream BamD fragment, which terminates 28 bp upstream of *F108* (Fig. 2B), was also supported by inspection of the codon usage in the region upstream from *F108* as well as by the mutational and transcriptional analyses described below. This region will be termed *F0* in this study. Based on these results and on the mutational and complementation analysis described below, we conclude that there are four ORFs within the BamF fragment located upstream from the *puhA* gene. These, by convention, are designated *F0*, *F108*, *F1025*, and *F1696*.

**Interposon mutagenesis of *F0*, *F108*, and *F1025*.** Interposon mutagenesis of *F0*, *F108*, and *F1025* was undertaken through the insertion of a Km<sup>r</sup> cassette into the chromosome at sites located within each of the respective genes (Fig. 4) (Materials and Methods). A strain containing an insertion mutation in *F0* (ZY6) was constructed by recombining a Km<sup>r</sup> cassette into the chromosome at the *Bam*HI site located at the BamD-BamF junction. Spectral analysis of photopigments accumulated by ZY6 demonstrated a complete loss of peaks above  $A_{500}$ , which is characteristic of a mutation that blocks BChl biosynthesis early in the pathway (Fig. 5A) (5). Fluorescence emission spectra of extractable pigments accumulated by ZY6 showed a photopigment with an emission maximum at 635 nm (Fig. 5B) but no obvious migration in silica gel TLC (Table 2) developed in benzene-ethyl acetate-ethanol (4:1:1). This is characteristic of an increased accumulation of protoporphyrin IX (5); indeed, the tetrapyrrole accumulated by ZY6 was identical in all respects (such as the amounts of tetrapyrroles synthesized and their absorbance, emission, and chromatographic properties) to the photopigment accumulated in strain BRP50 (Table 2). This strain has previously been shown to accumulate protoporphyrin IX as a result of a mutation of the *bchH* gene (5). From these data, as well as for the complementation results discussed below, we conclude that *F0* encodes the carboxyl-terminal portion of the *bchH* gene.

An interposon deletion of *F108* was constructed by replacing an internal 54-bp *Pst*I restriction fragment in *F108* with a Km<sup>r</sup> cassette as described in Materials and Methods. Strain ZY5, which contained this deletion, synthesized large amounts of photopigments with absorbance maxima in acetone-methanol (7:2) at 627 and 572 nm (Fig. 5A; Table 2). This absorbance profile is characteristic of *bchB* mutants (5, 18), which are known to accumulate protochlorophyllide and MPE; indeed, this strain formed the same amounts of tetrapyrroles with the same absorbance spectrum, fluorescence emission spectrum, and TLC properties as those of the pigments produced by the previously characterized *bchB* mutations Y80 and BPY4 (Table 2). The accumulation of MPE in these strains was confirmed by the fluorescence emission spectrum, which showed a major emission peak at 634 nm, which was slightly shifted from the 635-nm peak observed in ZY6 and by the observed migration of this photopigment in the TLC system employed (Table 2) (5). These strains also accumulated trace amounts of magnesium-protoporphyrin IX, which is observed as a smaller emission peak at 595 nm. From these data we conclude that *F108* most likely encodes one of the protein subunits involved in the conversion of protochlorophyllide to chlorophyllide a.

A interposon deletion of *F1025* was constructed by replacing an internal 156-bp *Eco*RV restriction fragment from *F1025* with the Km<sup>r</sup> cassette. Spectral analysis of ZY4, which contained this deletion, also shows an absence of an absorbance peak above 500 nm associated with this mutation

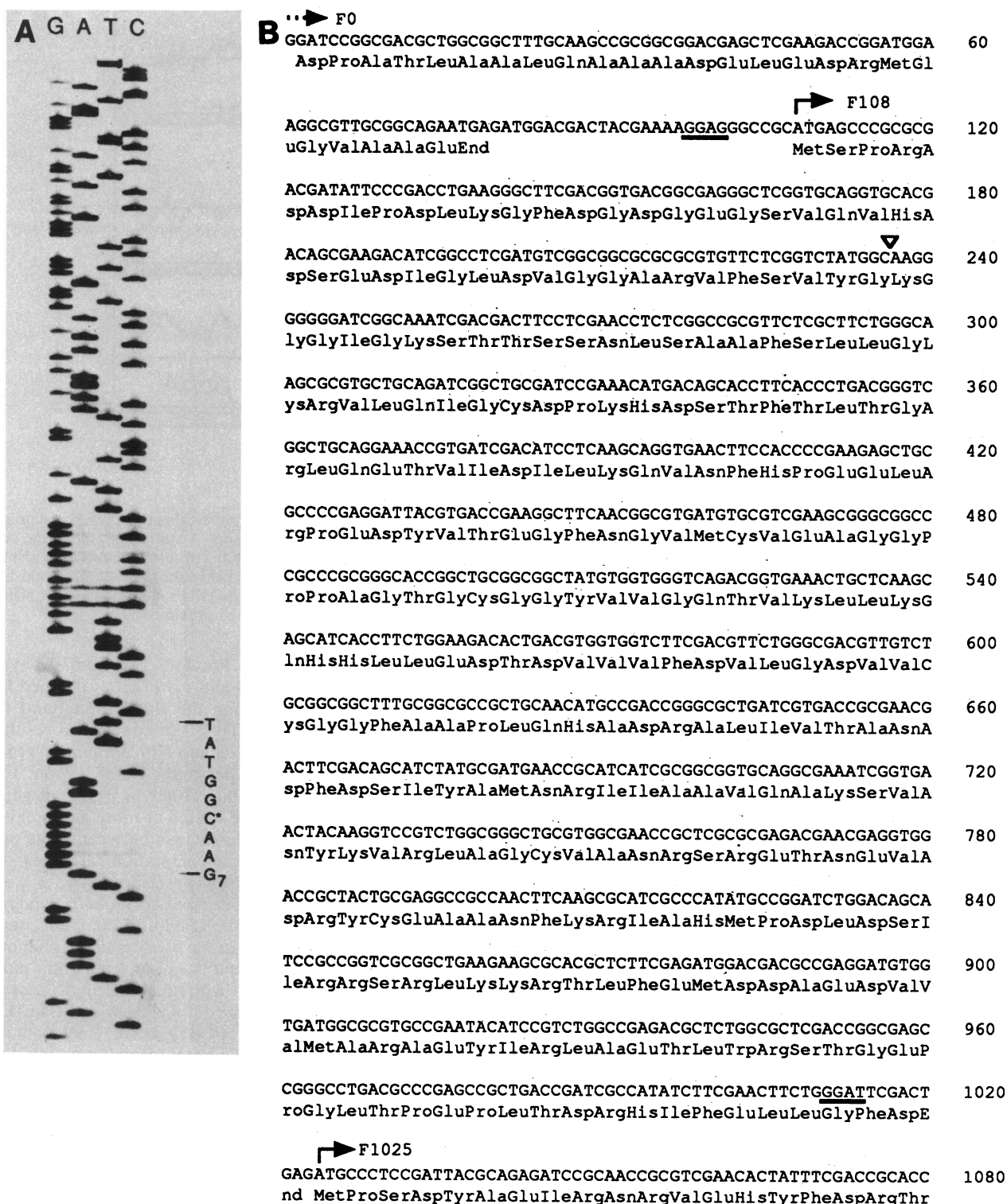


FIG. 2. Corrected DNA sequence of the *F108* gene. (A) Autoradiogram showing the region containing a sequencing error; the asterisk denotes the position of a single C. Sequence analysis of the other strand showed the occurrence of a single G (data not shown). (B) Correct translation of the *F108* ORF, which extends from position 108 to 1019 as well as for a translation of the *F0* ORF extending from base 2 through 76. Putative ribosome-binding sites for *F108* and *F1025* are underlined, and the position of the frame shift is shown as an open triangle. This sequence has been submitted to the GenBank/EMBL data libraries under accession number M34843.

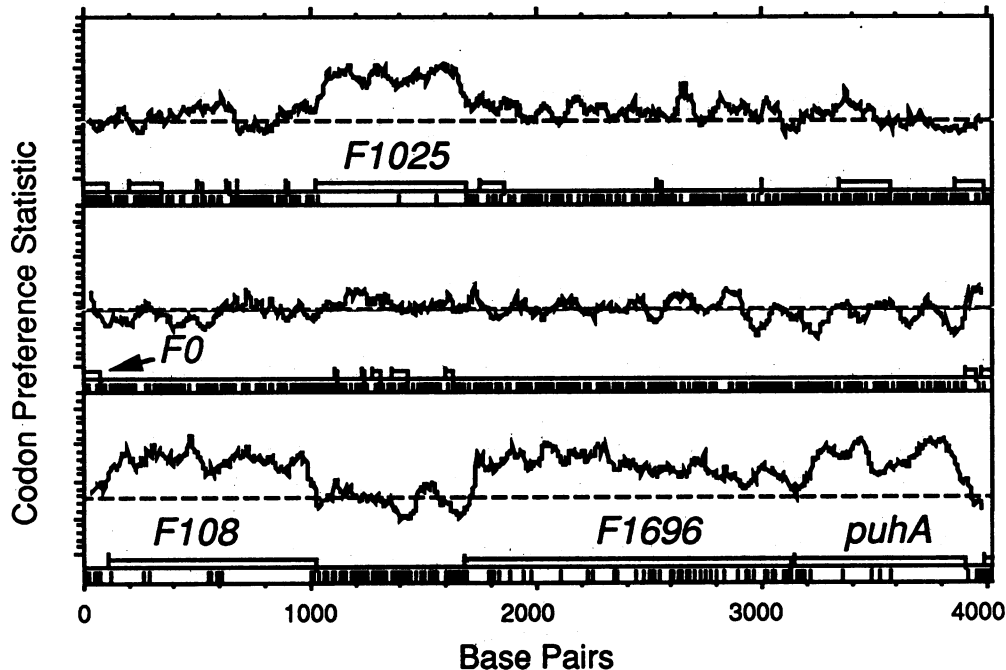


FIG. 3. Codon preference plot of the DNA sequence encoded by the BamF restriction fragment. The statistical codon preference program of Gribskov et al. (13) was used to confirm the potential existence of translated ORFs in the BamF region. A statistical plot of the codon utilization for each reading frame is shown in the three graphs, with each graph representing a different reading frame. The program identifies efficiently translated genes by virtue of ORFs (open boxes), which contain few rare codons (vertical dashes below the ORFs) and a good codon preference plot (a rise in the graph above random utilization, which is denoted as a dashed line). Each of the ORFs identified by this program are indicated. A codon utilization data base obtained from known *R. capsulatus* genes has been described previously (34).

(Fig. 5A). Fluorescence emission spectra, however, showed that ZY4 accumulated tetrapyrroles, exhibiting emission maxima at 595 and 634 nm; as discussed above, these spectra are characteristic of magnesium-protoporphyrin IX and MPE, respectively (Fig. 5B). This was further confirmed by the TLC properties exhibited by these photopigments (Table 2). The photopigments accumulated by ZY4 were also identical in their amounts, absorbance spectra, fluorescence emission spectra, and TLC properties to photopigments produced by the previously characterized *bchE* mutation BRP4 (Table 2) (5). From these results we conclude that *F1025* most likely encodes a polypeptide involved in the closure of the cyclopentone ring of MPE, forming protochlorophyllide.

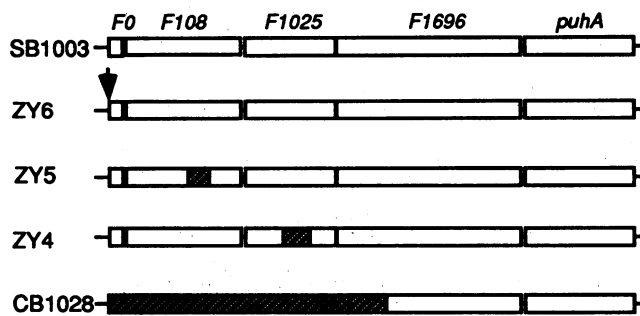


FIG. 4. Map of mutations created by site-directed mutagenesis. The diagram denotes the location of the  $Km^r$  cassette in differing ORFs present in the parent strain SB1003. The arrow in ZY6 denotes the location of an insertion mutation in *F0*. The hatched regions present in ZY5, ZY4, and CB1028 represent regions of DNA replaced by the  $Km^r$  cassette as described in the text.

**Complementation analysis.** Previous genetic and physical mapping studies of the *bchB* and *bchE* genes mapped locations for these genes to within the BamD and BamI fragments, respectively (5, 29). This is in contrast to results of our study, which mapped *F108* and *F1025* mutations exhibiting *bchB* and *bchE* phenotypes to the BamF region. These conflicting results could be due either to incorrect genetic mapping or to the occurrence of two or more genes exhibiting similar phenotypes. To distinguish between these possibilities, we performed complementation analyses with strains containing the interposons described above as well as with several previously characterized *bchH*, *bchE*, and *bchB* point mutations (Table 3). The results of complementation analysis with strains exhibiting a *bchH* mutant phenotype demonstrate that both ZY6 ( $F0::Km^r$ ) and the point mutant BRP50 are complemented with the plasmid construct pCB701D $\Omega$ , a construct that contains both the BamD and BamF fragments. In contrast, pCB701D $\Omega_0$ , which contained a gene interruption of *F0* at the BamD-BamF junction, failed to complement both mutations. These results support the conclusion that the  $F0::Km^r$  interruption disrupts the *bchH* gene.

The results of complementation analyses with strains exhibiting a *bchB* mutant phenotype also demonstrate that pCB701D $\Omega$  complements all mutations exhibiting this phenotype. However, a plasmid construct containing only the BamF fragment (pCB701 $\Omega$ ) exhibited marker rescue only with strains ZY5 ( $F108::Km^r$ ) and BPY4 but not with strains AJB478, AJB480, or Y80. This suggests the existence of two complementation groups exhibiting the *bchB* mutant phenotype, one including strains ZY5 and BPY4 and the other AJB478, AJB480, and Y80.

Similarly, ZY4 ( $F1025::Km^r$ ) and BRP4, which both ex-

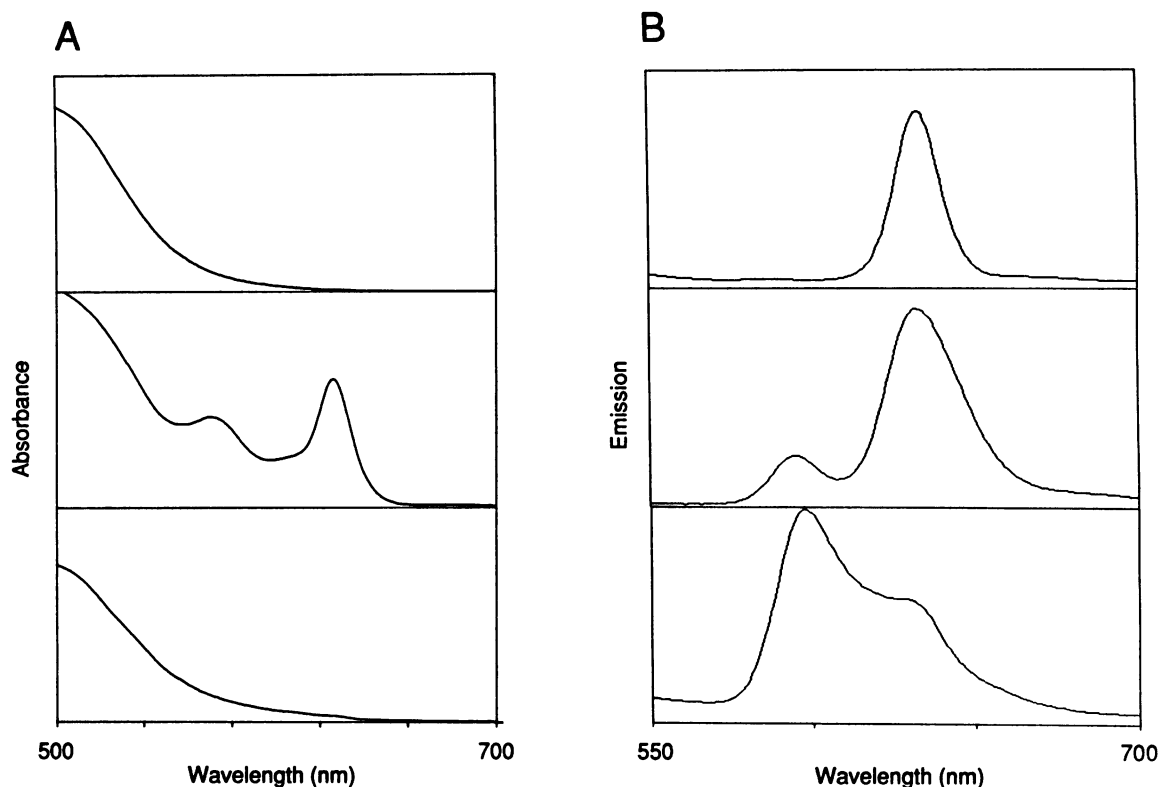


FIG. 5. Spectral and fluorescence analysis of tetrapyrroles accumulated as a result of mutations in *F0*, *F108*, and *F1025*. (A) Spectral analysis of accumulated tetrapyrroles extracted by acetone-methanol (7:2) in strains bearing a mutation in *F0* (ZY6, top), *F108* (ZY5, middle), and *F1025* (ZY4, bottom). (B) Fluorescence emission spectra of tetrapyrroles accumulated by strains ZY6 (top), ZY5 (middle), and ZY4 (bottom). The excitation wavelength for the emission spectra was set at 402 nm.

hibited an identical *bchE* mutant phenotype, also fell into two different complementation groups as demonstrated by the ability of pCB701D $\Omega$  to complement ZY4 but not BRP4 and by the ability of pRPSB9, a plasmid containing the BamI fragment (29), to complement BRP4 and not ZY4.

**Transcriptional analysis.** Several studies were undertaken to determine the size of the transcript responsible for expressing the genes characterized in this study and for the regulation of expression in response to changes in oxygen tension. The size of the transcript was estimated by complementation analysis and by Northern blot analysis. Complementation analysis was performed by first constructing a

2,424-bp deletion, extending from *F0* through *F1696*, which was constructed by substituting this region with a Km<sup>r</sup> cassette as described in Materials and Methods. CB1028, a strain bearing this deletion, exhibited no BChl biosynthesis and therefore cannot grow photosynthetically. CB1028 was subsequently assayed for complementation with plasmids that contain the BamF fragment as well as various amounts of the upstream BamD region. The results of this analysis (Fig. 6A) demonstrated that CB1028 can be fully complemented by a plasmid containing 7.5 kb (pCB701D $\Omega$ ) upstream from *F0* but not by plasmid constructs containing 4.5 kb (pCB701E $\Omega$ ) or 2.5 kb (pCB701F $\Omega$ ) of DNA upstream from *F0*. Taking into account the size of the BamF region, these results suggest that this region encompasses an operon between 7 and 11 kb of DNA. The length of the transcript was also assayed by Northern blot analysis with a plasmid probe (pZY32) encoding the *F0*, *F108*, and *F1025* genes. The results of the Northern blot analysis (Fig. 6B) demonstrated the presence of a mRNA transcript with an approximate size of 11 kb, based on gel mobility. Finally, a plasmid encoding a *F0*::*lacZ* translational fusion (pZY62 $\Omega$ ) was constructed to assay the effect of oxygen tension on expression of this operon. This plasmid construct, when assayed with a wild-type strain of *R. capsulatus* grown under aerobic conditions, produced 50 U of  $\beta$ -galactosidase activity. In contrast, when these cells were assayed under anaerobic conditions, expression was increased to 123 U of activity. Thus, expression of this operon appears to be slightly regulated (2.5-fold) by oxygen tension.

TABLE 2. Absorbance, emission, and TLC properties of tetrapyrroles synthesized by Bchl<sup>-</sup> strains<sup>a</sup>

Mutant strain	Absorbance peak (nm)	Emission peak (nm)	<i>R<sub>f</sub></i> (s)
Brp50 ( <i>bchH</i> )		635	0.0
ZY6 ( <i>F0</i> )		635	0.0
Bpy4 ( <i>bchB</i> )	627 <sup>b</sup> , 572	634 <sup>b</sup> , 595	0.61, 0.55, 0.51
Y80 ( <i>bchB</i> )	627 <sup>b</sup> , 572	634 <sup>b</sup> , 595	0.61, 0.55, 0.51
ZY5 ( <i>F108</i> )	627 <sup>b</sup> , 572	634 <sup>b</sup> , 595	0.61, 0.55, 0.51
Brp4 ( <i>bchE</i> )		595 <sup>b</sup> , 634	0.61, 0.51
ZY4 ( <i>F1025</i> )		595 <sup>b</sup> , 634	0.61, 0.51

<sup>a</sup> Absorbance and emission analyses were performed on pigments extracted and scanned in acetone-methanol (7:2) with the excitation wavelength for emission spectra set at 402 nm.

<sup>b</sup> Major absorbance or emission peak.

TABLE 3. Complementation analysis of Bchl mutations<sup>a</sup>

Plasmid	<i>bchH</i>		<i>bchB</i>				<i>bchE</i>		
	ZY6	BRP50	ZY5	BPY4	AJB478	AJB480	Y80	ZY4	BRP4
pCB701DΩ (BamF, BamD)	+	+	+	+	+	+	+	+	-
pCB701Ω (BamF)			(+)	(+)	-	-	-	(+)	-
pCB701DΩ0 (BamF, BamD; <i>F0</i> ::Sp <sup>r</sup> )	-	(+)							
pZY33 (BamF; <i>F108</i> ::Km <sup>r</sup> )			-	(+)	-	-	-		
pZY22 (BamF; <i>F1025</i> ::Km <sup>r</sup> )								-	-
pRPSB9 (BamI)								-	+

<sup>a</sup> +, Complementation; (+), marker rescue; -, no complementation or marker rescue observed. Complementation and marker rescue were assayed as described by Young et al. (34). Plasmids and strains are discussed in the text.

## DISCUSSION

The results of this study demonstrate that the BamD and BamF fragments of the photosynthetic gene cluster encodes a large operon that contains numerous genes involved in Bchl biosynthesis. Complementation analyses performed in this and previous studies (5, 29, 36), suggest that this region may encode as many as six genes involved in five early stages of the Bchl *a* biosynthetic pathway (Fig. 1). Several of our results suggests that the BamF fragment contains for three transcribed ORFs, termed *F0*, *F108*, *F1025*, that encode polypeptides involved in the formation of MPE, chlorophyllide, and protochlorophyllide, respectively. The evidence for the existence of these genes is based, in part, on the excellent codon preference profile of these ORFs as assayed with the codon preference program by Gribskov et al. (13). In the past, this program has faithfully identified transcribed regions of the *puf*, *bchCA*, and *crtEF* operons (3, 34) and genes encoded by *puhA*, *puc*, *pet*, and *nifHD* operons (unpublished data). In no cases have we observed this program to incorrectly fuse two or more known ORFs to embed one ORF within another. The genetic evidence discussed below, which demonstrated that each of these interruptions causes a different phenotype, provides additional evidence for the transcription of these ORFs. Based on these results, as well as those of Zsebo and Hearst (36), we propose to rename *F108* as *bchL* and *F1025* as *bchM*, thereby giving an operon designation as *bchBFKHLM-F1696*.

Although we cannot rule out the possibility of polar effects of the Km<sup>r</sup> insertions created in this study, we feel that it is

highly unlikely for the following reasons. Foremost is the observation that each of these mutations results in a different phenotype, which would not be the case if these insertions were polar (as noted in Materials and Methods, the Km<sup>r</sup> gene used in this study is not flanked by transcription termination signals). For example, the argument against polarity for the *F108* mutation is based on the observation that the *F1025* gene product acts earlier in the pathway than does the upstream *F108* gene product. Therefore, if the *F108* disruption were causing a polar effect on expression of *F1025*, then it would be expected that this mutation would have a similar phenotype as the *F1025* disruption. For *F108* this is clearly not occurring. An argument for polarity of the *F1025* mutation on expression of *F1696* and *puhA* can also be made; however, we feel that it is unlikely for two reasons. (i) A deletion of *F1696* by interposon mutagenesis does not affect pigment biosynthesis (unpublished data) and therefore cannot be responsible for the phenotypes described in this study. (ii) We observed full complementation of mutations constructed in this study to a wild-type phenotype by the addition of the plasmid pCB701DΩ, which contains the BamD region as well as *F0* through *F1696* genes but not the *puhA* gene (data not shown). Since this plasmid complements the mutations, there appears to be no significant effect of the insertions on expression of the chromosomal copy of *puhA*.

Several of our results suggests that insertion of the Km<sup>r</sup> cassette into the BamHI site located at the BamD-BamF junction is disrupting the previously characterized *bchH* gene. This insertion causes a phenotype that is indistinguish-

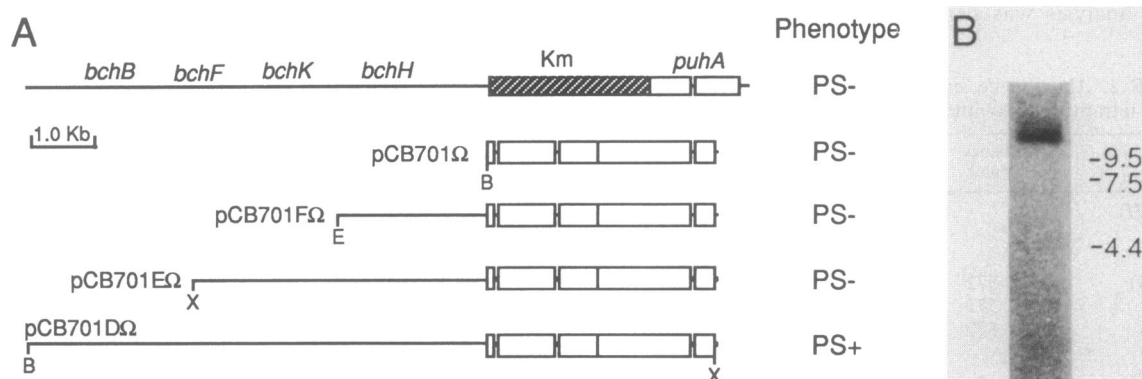


FIG. 6. (A) Analysis of transcript size by complementation. The top line is a schematic diagram of strain CB1028 in which the region of the chromosome containing ORFs *F0* through *F1696* has been replaced by a cassette encoding for Km<sup>r</sup>. As indicated, this strain is unable to grow photosynthetically (PS<sup>-</sup>). The remaining lines denote ability of the diagramed plasmids to complement the deletion in CB1028. Restriction fragment abbreviations are as described in Fig. 1. (B) Analysis of transcript size by Northern blot. Total RNA isolated from photosynthetically grown cells was separated by size and probed for mRNA encoding for the *F0* through *F1696* region as described in the text.



able to that observed for the *bchH* mutation in strain BRP50, which is in the same complementation group. Inspection of the DNA sequence upstream from *F108* demonstrates the existence of an ORF exhibiting excellent codon usage that extends 76 bp into the BamF region. Further evidence for transcription of this gene is based on the results of our analysis, which demonstrates that an *F0::lacZ* translational fusion is expressed and regulated in amounts comparable to those in similar fusions of the *bchC* gene to *lacZ* (34). In addition, constructs that contain translational fusions of *F0* to *lacZ* in the other two reading frames show no detectable  $\beta$ -galactosidase activity (data not shown). It has previously been proposed that the *bchH* gene encodes for a polypeptide that is responsible for magnesium chelatase activity that catalyzes the insertion of Mg into the tetrapyrrole or for the methyl transferase activity that catalyzes the transfer of a methyl group from *S*-adenosylmethionine to the propionic acid group of position 6 in the tetrapyrrole (5, 10). This is based on the observation that disruption of this gene results in the accumulation of protoporphyrin IX. It is as yet unclear which, if either, of these reactions this polypeptide may be catalyzing, since a detailed investigation of the presence or absence of these activities in these strains, which is beyond the scope of this study, has not yet been undertaken. Since mutations within this gene appears to disrupt the pigment pathway at the branch point from heme biosynthesis, it is just as likely that this polypeptide may instead play a regulatory role analogous to that proposed for the PufQ polypeptide (2).

A mutation in *F108*, which is in the same complementation group as the previously described point mutation BPY4, results in the accumulation of protochlorophyllide, suggesting that *F108* encodes a subunit of the enzyme that catalyzes the *trans* reduction of ring D to form chlorophyllide *a*. From fluorescence emission spectra at  $-70^{\circ}\text{C}$  (unpublished observations), the protochlorophyllide appears to be a mixture of monovinyl and divinyl protochlorophyllide, with divinyl dominating (ratios of monovinyl to divinyl protochlorophyllide, 0.14 for ZY5 and 0.31 for Y80). Mixtures of monovinyl and divinyl protochlorophyllide have been previously observed in plant studies (4, 23), and recent evidence suggests that the monovinyl and divinyl derivatives of protochlorophyllide may be intermediates in divergent pathways that lead to monovinyl and divinyl derivatives of Chl *a* (23). The polypeptide encoded by *F108* exhibits no obvious sequence similarity to the light-dependent protochlorophyllide oxidoreductase gene product from barley (26). Both of these enzymes appear to catalyze similar reactions; however, the reaction in the higher plant requires a light activation step that is not found in bacteria, suggesting that it may be unrelated. This possibility is supported by the observation that *Chlorella* sp. appears to have two separate enzymes catalyzing this reaction, one which is light dependent and another which is light independent (14).

A mutation in *F1025* inhibits the conversion of MPE to protochlorophyllide. This part of the pathway involves a rather complex closure of the cyclopentone ring, which most likely involves several enzymatic reactions (4, 7). Failure to detect any intermediates between MPE and protochlorophyllide in this or other mutational studies suggests either that such intermediates are unstable or that the formation of the cyclopentone ring may involve a multifunctional enzyme complex that loses all activity when mutated. Results of the complementation analysis demonstrate that more than one polypeptide subunit is, indeed, involved in the conversion of MPE to protochlorophyllide. Whether they are subunits of a

single or multiple enzyme complex will have to await further analysis.

More detailed information on these reactions, in both plant and bacterial systems, will require characterization of the catalytic polypeptides. However, isolation of enzymes catalyzing these events has been hampered due to inherent difficulty in observing appreciable *in vitro* activities. Thus, our genetic approach provides some unique structural information on proteins involved in the early stages of pigment biosynthesis for bacterial or plant systems. Despite observations that indicate association of these enzymes with the membrane fraction (4, 6, 7, 12, 16, 23, 28), analysis of the polypeptide sequences encoded by *F0*, *F108*, and *F1025* indicate very few hydrophobic residues, and a hydrophobicity plot shows no obvious membrane-spanning regions (17). This raises the possibility that the polypeptides are only peripherally associated with the membrane fraction. Further insight to these reactions could be gained from a phylogenetic study of comparable genes from plant systems. Such an analysis would provide information about conserved structural features in proteins catalyzing these reactions as well as for the evolutionary relationship between bacterial and plant photosynthesis. The sequence information provided by this study should facilitate such efforts.

#### ACKNOWLEDGMENTS

We thank Constantine Rebiz for calculating the monovinyl and divinyl ratios of protochlorophyllide reported in this study and to Howard Gest and members of the Photosynthetic Bacteria Group for critical reading of the manuscript. We especially thank J. Favinger for technical assistance.

This work was supported by Public Health Service grant GM40941-01 from the National Institutes of Health.

#### LITERATURE CITED

1. Barany, F. 1985. Single-stranded hexameric linkers: a system for in phase insertion mutagenesis and protein engineering. *Gene* 37:111-123.
2. Bauer, C. E., and B. L. Marrs. 1988. *Rhodobacter capsulatus* *puf* operon encodes a regulatory protein (PufQ) for bacteriochlorophyll biosynthesis. *Proc. Natl. Acad. Sci. USA* 85:7074-7078.
3. Bauer, C. E., D. A. Young, and B. L. Marrs. 1988. Analysis of the *Rhodobacter capsulatus puf* operon. *J. Biol. Chem.* 263:4820-4827.
4. Beale, S. I. 1984. Biosynthesis of photosynthetic pigments, p. 133-205. In N. R. Baker and J. Barber, (ed.), *Chloroplast biogenesis*. Elsevier Science Publishing, Inc., New York.
5. Biel, A. J., and B. L. Marrs. 1983. Transcriptional regulation of several genes for bacteriochlorophyll biosynthesis in *Rhodospseudomonas capsulata* in response to oxygen. *J. Bacteriol.* 156:686-694.
6. Castelfranco, P. A., and S. I. Beale. 1981. Chlorophyll biosynthesis, p. 375-421. In M. D. Hatch and N. K. Boardman (ed.), *The biochemistry of plants*, vol. 8. Academic Press, Inc. New York.
7. Castelfranco, P. A., and S. I. Beale. 1983. Chlorophyll biosynthesis: recent advances and areas of current interest. *Annu. Rev. Plant Physiol.* 34:241-278.
8. Clayton, R. K. 1966. Spectroscopic analysis of bacteriochlorophylls *in vitro* and *in vivo*. *Photochem. Photobiol.* 5:669-677.
9. Gaugh, J. A., and N. E. Murray. 1983. Sequence diversity among related genes for recognition of specific targets in DNA molecules. *J. Mol. Biol.* 166:1-19.
10. Gorchein, A. 1972. Magnesium protoporphyrin chelatase activity in *Rhodospseudomonas sphaeroides*. Studies with whole cells. *Biochem. J.* 127:97-106.
11. Granick, S. 1950. The structural and functional relationships

- between heme and chlorophyll. *Harvey Lect.* **44**:220–245.
12. **Granick, S., and S. I. Beale.** 1978. Hemes, chlorophylls, and related compounds: biosynthesis and metabolic regulation. *Adv. Enzymol.* **46**:33–203.
  13. **Gribskov, M., J. Devereaux, and J. Burges.** 1984. The codon preference plot: graphic analysis of protein coding sequences and prediction of gene expression. *Nucleic Acids Res.* **12**:539–547.
  14. **Griffiths, W. T., and R. E. Mapleston.** 1978. NADPH-protochlorophyllide oxidoreductase. p. 99–105. *In* G. Akoyunoglou and J. H. Argyrbudi-Akoyunoglou (ed.), *Chloroplast development*. Elsevier/North-Holland Publishing Co., Amsterdam.
  15. **Hanahan, D.** 1983. Studies on transformation of *Escherichia coli* with plasmids. *J. Mol. Biol.* **166**:557–580.
  16. **Jones, O. T. G.** 1978. Biosynthesis of porphyrins, hemes and chlorophylls, p. 751–777. *In* R. K. Clayton and W. R. Sistrom (ed.), *The photosynthetic bacteria*. Plenum Publishing Corp., New York.
  17. **Kyte, J., and R. F. Doolittle.** 1982. A simple method for displaying the hydrophobic character of a protein. *J. Mol. Biol.* **157**:105–132.
  18. **Lascalles, J.** 1966. The accumulation of bacteriochlorophyll precursors by mutant and wild type strains of *Rhodospseudomonas sphaeroides*. *Biochem. J.* **100**:175–183.
  19. **Marrs, B. L.** 1981. Mobilization of the genes for photosynthesis from *Rhodospseudomonas capsulatus* by a promiscuous plasmid. *J. Bacteriol.* **146**:1003–1012.
  20. **Messing, J., and J. Vieira.** 1982. A new pair of M13 vectors for selecting either DNA strand of double-digest restriction fragments. *Gene* **19**:269–276.
  21. **Minton, N. P.** 1984. Improved plasmid vectors for the isolation of translational *lac* gene fusions. *Gene* **31**:269–273.
  22. **Prentki, P., and H. M. Krisch.** 1984. In vitro insertional mutagenesis with a selectable DNA fragment. *Gene* **29**:303–313.
  23. **Rebeiz, C. A., and J. Lascalles.** 1982. Biosynthesis of pigments in plants and bacteria, p. 699–779. *In* Govindjee (ed.), *Photosynthesis: energy conversion by plants and bacteria*. Academic Press, Inc., New York.
  24. **Sambrook, J., E. F. Fritsch, and T. Maniatis.** 1989. *Molecular cloning: a laboratory manual*. Cold Spring Harbor Laboratory, Cold Spring Harbor, N.Y.
  25. **Sanger, F., S. Nicklen, and A. R. Coulson.** 1977. DNA sequencing with chain-terminating inhibitors. *Proc. Natl. Acad. Sci. USA* **74**:5463–5467.
  26. **Schulz, R., K. Steinmuller, M. Klaas, C. Forreiter, S. Rasmussen, C. Hiller, and K. Apel.** 1989. Nucleotide sequence of a cDNA coding for the NADPH-protochlorophyllide oxidoreductase (PCR) of barley (*Hordeum vulgare* L.) and its expression in *Escherichia coli*. *Mol. Gen. Genet.* **217**:355–361.
  27. **Scolnik, P. A., and R. Haselkorn.** 1984. Activation of extra copies of genes coding for nitrogenase in *Rhodospseudomonas capsulata*. *Nature (London)* **307**:289–292.
  28. **Smith, B. B., and C. A. Rebeiz.** 1979. Chloroplast biogenesis. XXIV. Intrachloroplastic localization of the biosynthesis and accumulation of protoporphyrin IX, magnesium-protoporphyrin monoester, and longer wavelength metalloporphyrins during greening. *Plant Physiol.* **63**:227–231.
  29. **Taylor, D. P., S. N. Cohen, W. G. Clark, and B. L. Marrs.** 1983. Alignment of genetic and restriction maps of the photosynthesis region of the *Rhodospseudomonas capsulata* chromosome by a conjugation-mediated marker rescue technique. *J. Bacteriol.* **154**:580–590.
  30. **Viera, J., and J. Messing.** 1982. The pUC plasmids, an M13mp7-derived system for insertion mutagenesis and sequencing with synthetic universal primers. *Gene* **19**:259–268.
  31. **Weaver, P. F., J. D. Wall, and H. Gest.** 1975. Characterization of *Rhodospseudomonas capsulata*. *Arch. Microbiol.* **105**:207–216.
  32. **Wellington, C. L., and J. T. Beatty.** 1989. Promoter mapping and nucleotide sequence of the *bchC* bacteriochlorophyll biosynthesis gene from *Rhodobacter capsulatus*. *Gene* **83**:251–261.
  33. **Yen, H. C., and B. L. Marrs.** 1976. Map of genes for carotenoid and bacteriochlorophyll biosynthesis in *Rhodospseudomonas capsulata*. *J. Bacteriol.* **126**:619–629.
  34. **Young, D. A., C. E. Bauer, J. C. Williams, and B. L. Marrs.** 1989. Genetic evidence for superoperonal organization of genes for photosynthetic pigments and pigment-binding proteins in *Rhodobacter capsulatus*. *Mol. Gen. Genet.* **218**:1–12.
  35. **Youvan, D. C., E. J. Bylina, M. Alberti, H. Begusch, and J. E. Hearst.** 1984. Nucleotide and deduced polypeptide sequences of the photosynthetic reaction-center, B870 antenna, and flanking polypeptides from *R. capsulata*. *Cell* **37**:949–957.
  36. **Zsebo, K. M., and J. E. Hearst.** 1984. Genetic-physical mapping of a photosynthetic gene cluster from *R. capsulata*. *Cell* **37**:937–947.